Available online at www.sciencedirect.com
ScienceDirect
Advances in Space Research 48 (2011) 218–226
ADVANCES IN SPACE RESEARCH
(a COSPAR publication)
www.elsevier.com/locate/asr

Simultaneous bi-station measurements of mesospheric waves from Indian low latitudes

Alok Taori [a,*], Navin Parihar [b]

[a] National Atmospheric Research Laboratory, Gadanki, Andhra Pradesh 517 112, India
[b] Indian Institute of Geomagnetism, Allahabad, Uttar Pradesh 221 505, India

Received 27 October 2010; received in revised form 14 March 2011; accepted 22 March 2011
Available online 27 March 2011

Abstract

Coordinated mesospheric night-airglow measurements have been carried out from two stations, Gadanki (13.5° N, 79.2° E) and Allahabad (25.5° N, 81.9° E), India during April 2009 to study the common gravity wave features. With two nights of coordinated measurements we find some of the wave periodicities to be similar at the two locations. Simultaneous OH and O_2 intensity measurements over Gadanki reveal these features to be upward propagating gravity waves while the coordinated OH intensity measurements of similar waves from Allahabad show the large spatial extent of these waves.

Keywords: Mesosphere; Gravity wave; Propagation; Dissipation

1. Introduction

Atmospheric gravity waves play an important role in transferring energy and momentum from one atmospheric region to other which, in-turn affects mesosphere and lower thermosphere (MLT) region processes (e.g., Fritts and Alexander, 2003). It is our growing understanding that these waves have their source regions located at tropospheric altitudes and any sudden change brought into the tropospheric altitudes has the potential to generate a spectrum of gravity wave. For example, the passage of wind over topographic structures, weather fronts, convective activity, and wind shears are plausible sources of gravity waves (e.g., Fritts and Alexander, 2003 and references cited therein). It is also understood that these gravity waves deposit their energy in the environment through linear and non-linear processes such as, wave breaking and insta-b-il-i-ti-es (e.g., Lindzen, 1981; Li et al., 2005) wave–wave and wave–mean flow interactions (Yeh and Liu, 1981; Fritts, 1985). These dissipation processes define the vertical and horizontal propagation limits of the wave.

Depending on the horizontal and vertical scales, these gravity waves propagate in oblique direction from their source regions. The distances traveled by these waves depend on the background conditions and wavelengths associated with the waves. Some of the recent observations of waves coming from far regions concern spectacular wave events known as mesospheric bores (Taylor et al., 1995) together with another strong mesospheric wave event (Smith et al., 2006 and references cited therein). They suggest that Doppler (or thermal) ducting may extend the spatial scales of these waves to several thousands of kilometers. However, Shiokawa et al. (2000) suggest the possibility of such waves propagating from the lower atmosphere to greater heights with increasing spatial scales which may be observed and noted as plane wave fronts at mesospheric altitudes. It is therefore suggested that with the help of single or close by co-located measurements it is difficult to understand if an upward propagating wave can h-a-

* Corresponding author. Address: National Atmospheric Research Laboratory, Gadanki, Pakala Mandal, Andhra Pradesh 517112, India. Tel.: +91 8585 272120; fax: +91 8585 272018.
E-mail addresses: alok.taori@gmail.com, taori@narl.gov.in (A. Taori).

0273-1177/$36.00 © 2011 COSPAR. Published by Elsevier Ltd. All rights reserved.
doi:10.1016/j.asr.2011.03.026

ve such large spatial coverage. Therefore, it is important to carry out measurements from distant locations. Further, because such waves have planer wave fronts at mesospheric altitudes and hence may trigger the generation of associated polarization electric fields at low latitude E-region altitudes and in-turn have important repercussions for the thermosphere–ionosphere system (e.g., Fritts et al., 2008; Tsunoda, 2010).

In this study we present the first such measurements from Gadanki (13.5° N, 79.2° E) and Allahabad (25.5° N, 81.9° E) stations in India. Though, there is a latitudinal difference of about 12° (radial distance ∼1200 km), investigation show commonality in the observed wave features.

2. Instrument and observations

In this report we utilize (a) intensity measurements at OH (6-2) and O_2 (0-1) wavelengths over Gadanki (13.5° N, 79.2° E), made with the help of a Mesosphere Lower Thermosphere Photometer (MLTP) and (b) OH intensity measurements made with the aid of an All Sky Imager at Allahabad (25.5° N, 81.9° E).

2.1. Mesosphere lower thermosphere photometer (MLTP)

The MLTP is a photomultiplier based narrow field (full field of view 4°) photometer with F/2 optics. The MLTP measures OH, O_2, O(^{1}D) and background (at 858 nm) emissions near simultaneously with a time resolution of ∼3 min. The interference filters have full width at half maxima (FWHM) of ∼0.4 nm. For the present study we utilize the calculated band intensities for OH (6-1) and O_2 (0-1) band emissions. The details of the instrument and analysis procedure are discussed elsewhere (e.g., Guharay et al., 2009; Taori et al., under review). The standard errors in the intensity estimates arising mainly from the dark counts and read-out noise of the photomultiplier tube are less than 0.05%, while the precision of measurement is ∼15–20 photon counts which assure high quality night airglow emission intensity measurements.

2.2. All sky imager (ASI)

The nightglow observations at Allahabad were carried out using a CCD based all sky imager (manufactured by Keo Scientific Ltd., Canada). The details of the imaging system are presented elsewhere (e.g., Mukherjee et al., 2010) while the adopted image processing is similar to Taylor et al. (1991). The image processing involved (a) flat-field corrections to account for the intensities variations due to lens curvature, (b) to approximately remove artifacts due to the van Rhijn effect and atmospheric extinction, (c) the non-uniform pixel-to-pixel sensitivity of the CCD detector, and (d) scaling to 5–95% of the intensity range. Later, assuming the OH emission peak to be at 87 km, the images were then transformed to a geographic coordinate system. Though, in general, this six-filter all sky imager takes observations at OH, O (^{1}S) and background (at 530 nm), during April 21–24, 2009 it was operated only at OH wavelengths. For OH measurements, a 190 nm broadband optical filter (720–910 nm) with 87% transparency was used, with a notch at 868 nm to exclude the contribution from the O_2 (0, 1) Atmospheric band emission. The signal to noise ratio of the imager is ∼200 for a time integration of 2 min that translates into a negligible (<0.05%) error in the intensity estimates. The exposure time used in this study is ∼2 min. In this study we utilize the average intensity of a 16 pixel × 16 pixel area corresponding to a square field of view of ∼3° at zenith (for the purpose of a fair comparison with MLTP observations).

2.3. Observations

The top panel in Fig. 1 plots the intensity variability of mesospheric OH and O_2 emissions over Gadanki while the bottom panel shows the OH intensity variability observed over Allahabad on 21–22 April 2009. The *x*-axis in each plot shows the Indian standard time IST) in hours in each

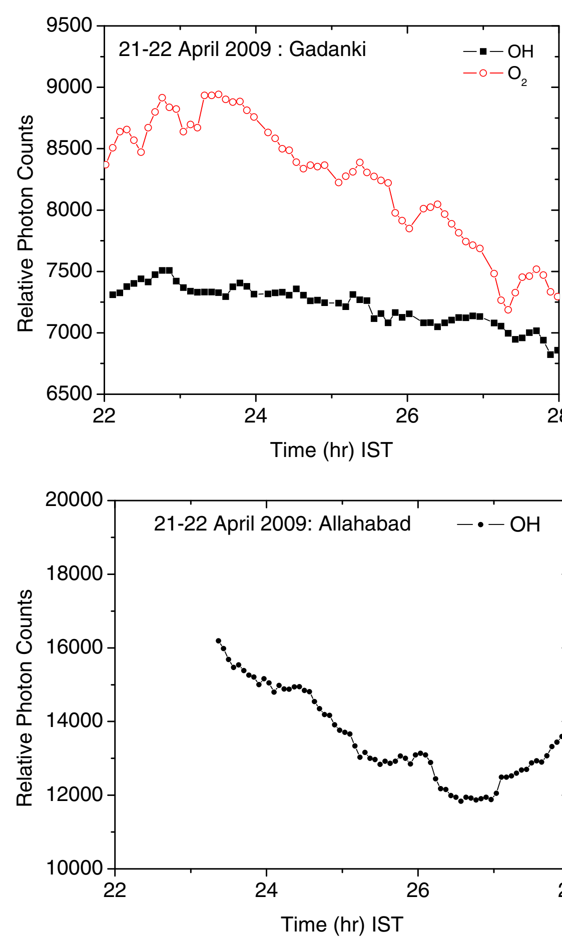

Fig. 1. Mesospheric airglow measurements from Gadanki (13.5° N, 79.2° E) (top panel) and Allahabad (25.5° N, 81.9° E) (bottom panel) on 21–22 April 2009. One may note signatures of small period waves together with a large period nocturnal trend in both the data.

plot. One may note a post evening decrease in the emission intensity for Gadanki as well as for the Allahabad data. It is also observed that Gadanki as well as Allahabad data are dominated by a long period wave embedded with other shorter period oscillatory features. Also, the long period nocturnal trend shows peak-to-peak intensity variability in OH and O_2 emissions over Gadanki to be ~10% and 18%, respectively, while over Allahabad the peak-to-peak intensity variability is ~20% for the OH emissions.

The observed intensity variations on 23–24 April 2009 are summarized in Fig. 2. On this night, Gadanki data (top panel) do not reveal a post evening decay while Allahabad data (bottom panel) does. It can be noted that intensity levels of OH emissions are almost half of those observed on 21–22 April 2009 at both the locations. Further, there are remarkable differences in the pattern of nocturnal variability observed over Gadanki and Allahabad. The Gadanki data shows sudden jumps and sharp variability in both, the OH and O_2 intensity data whereas these are not evident in Allahabad OH intensity data.

3. Results

As noted in Figs. 1 and 2, the nocturnal intensity variability over Gadanki and Allahabad exhibit somewhat distinct behavior. Further, it is obvious that the nocturnal variation of nighttime mesospheric airglow intensity (in general) on both the nights is a combination of a variety of waves which have short as well as long periodicities. Therefore, in order to investigate the common waves, we separate out the long period and short period waves from the observed variability as explained below.

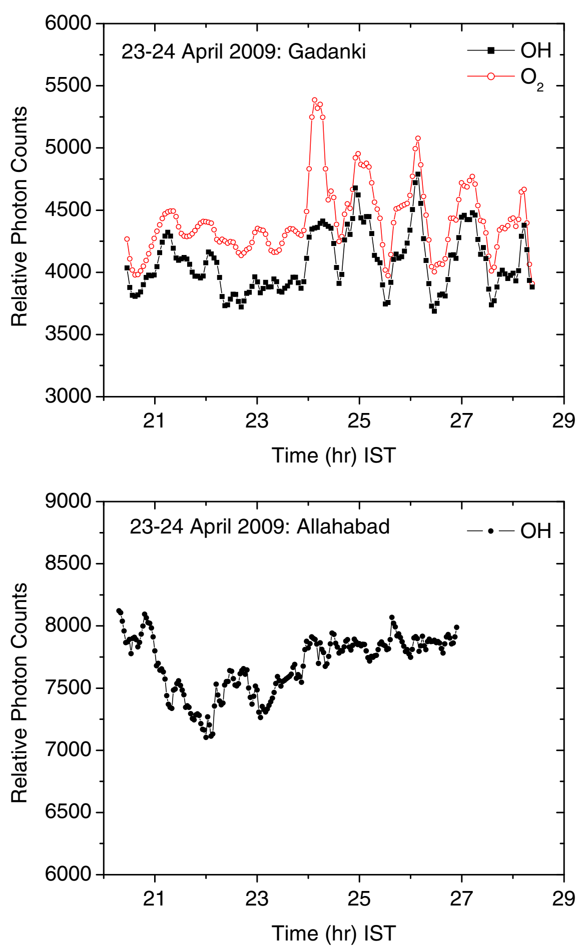

Fig. 2. Same as Fig. 1 but for 23–24 April 2009.

To estimate the long period feature, we fit the data with a simple sinusoidal model. Because only OH emission intensities are observed at the two locations simultaneously, we carry out a detailed analysis only for OH data. The results of this best-fit model are shown in Fig. 3 for the OH data of both the locations. The top panels in the figure plot the mean intensity deviations together with the best-fit results for Gadanki, while the bottom panels show mean intensity deviations and the resultant best-fit curves for Allahabad data on both the nights accordingly (i.e. 21–22 and 23–24 April 2009). On 21–22 April 2009, the best-fit analysis reveals the presence of ~12 h wave periodicity as the long period wave at both the locations, which emphasizes the presence of a semi-diurnal type wave at Gadanki as well as Allahabad. On the contrary, the 23–24 April 2009 data yield a poor fit for the long period waves which suggests the dominance of shorter period waves at both the locations. In fact, on this night, data exhibit a shorter period wave (~3 h) dominating the nocturnal pattern of variability at both the locations. Overall, the 23–24 April 2009 variability was characterized by the dominance of short period gravity waves while the 21–22 April 2009 variability exhibits the dominance of a semi-diurnal type wave.

Further, because our aim is to investigate the short period gravity wave features in the nocturnal data, to enhance the shorter period wave a 3 h running average has been detrended from the intensity data. Later, to explain and quantify the observed residual intensity variability of shorter period waves, a parametric best fit model which uses three sinusoidal components has been utilized. The selections of the sinusoidal components are based on the Lomb–Scargle periodogram method where only the three most dominant periods are selected for the best-fit modeling. The descriptions of the wave characteristics observed on both the nights are as follows.

3.1. 21–22 April 2009

Fig. 4 show the results of the parametric best-fit sinusoidal estimation for 21–22 April 2009. From top to bottom, we plot the results of residual intensity of Gadanki-O_2, Gadanki-OH and Allahabad-OH data, respectively. The top panels of each plot show the residual intensity data (filled circles and connecting lines) together with the best-fit results (solid lines) and the 90% confidence band of the model prediction. The bottom panels of each plot show the amplitude variability of the best-fit sinusoidal wave components. One may note the presence of some common wave features at both altitudes in the Gadanki data. The OH data over Gadanki is characterized by ~2, 1.3 and

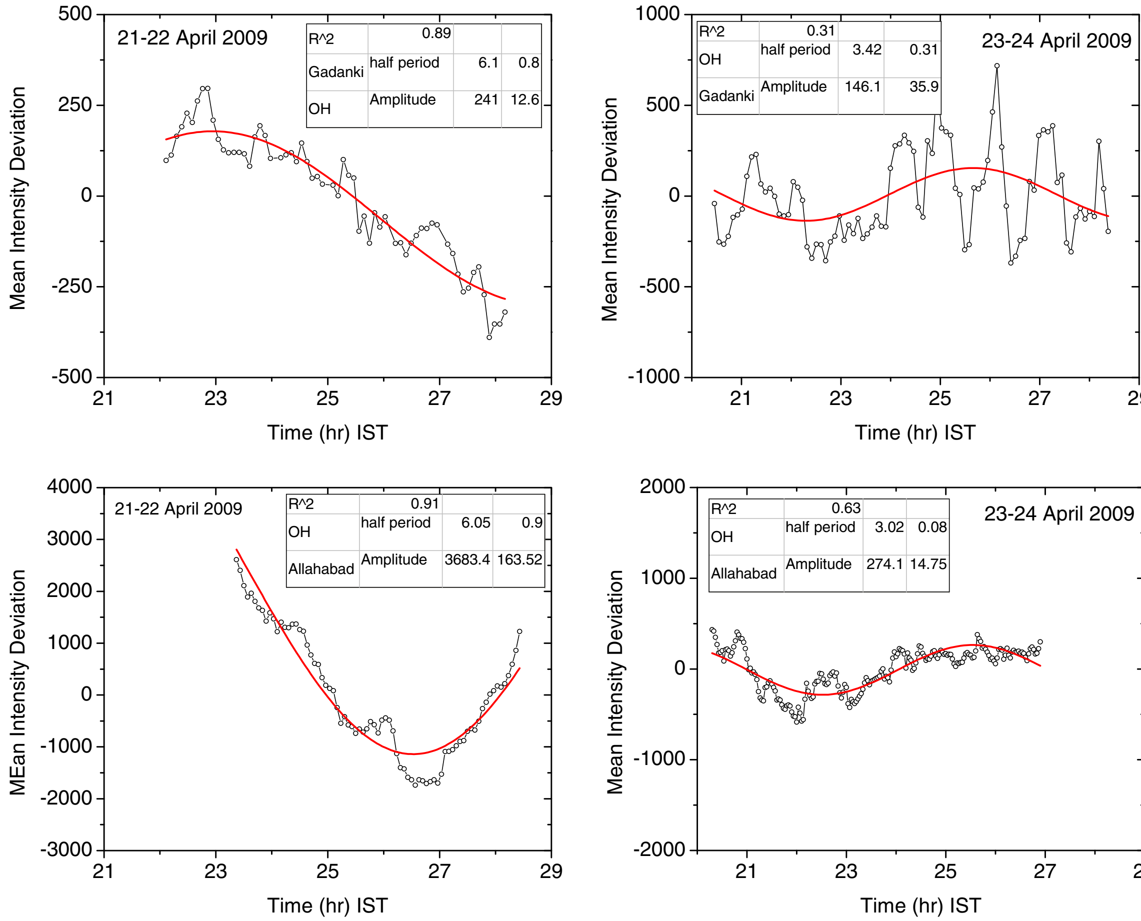

Fig. 3. The mean intensity deviations for the OH airglow emission for Gadanki and Allahabad data (open circles with connecting lines). Top panels show the Gadanki data while the bottom panel shows the data corresponding to Allahabad. The solid red lines in each plot are the best-fit curves depicting the long period nocturnal waves. (For interpretation of the references to color in this figure legend, the reader is referred to the web version of this article.)

0.8 h waves whereas the O_2 data is dominated by waves with periodicities ~2 and 1.2 h together with an unresolved long period wave with periodicity ~10 h. The absence of the 0.8 h wave at higher altitudes signifies the possible dissipation of this wave before it could reach the O_2 altitudes. Further, the cross correlation analysis reveals the maximum correlation coefficient of ~0.84 with about 0.7 h time shift for O_2 data. This, indeed is a clear signature of upward wave propagation in OH and O_2 data. Assuming the separation between the OH and O_2 layers remains ~9 km, the vertical group velocity is estimated to be ~10 km/h. The Allahabad intensity data (bottom panel) also show that somewhat similar waves dominate the OH data. The periodicity of waves over Allahabad is found to be ~6.7, 1.4 and 0.8 h. Among them, important to note is the presence of ~1.3 and 0.8 h waves at both the locations (note that Gadanki data show that the 0.8 h wave did not propagate to higher altitudes). It should be mentioned here that in this study, small differences in observed wave periods are treated as insignificant because of the instrument limitation and complex behavior of the atmosphere. We assume the vertical group velocity represents an average vertical velocity of the wave packet of ~0.6 km/h. Under this assumption and taking the natural oscillation period to be ~6 min, we calculate the vertical and horizontal wavelengths of the observed common wave using the linear dispersion relation for propagating gravity waves (Hines, 1960) [i.e., $\cos\theta = T_{\text{BVperiod}}/T_{\text{wave-period}}$ and $\tan\theta = \lambda_x/\lambda_z$, where θ is the angle of propagation]. The estimated vertical and horizontal wavelengths of the 1.2 h wave (which is common at Gadanki and Allahabad) are ~14 and 168 km which results in a propagation angle of ~85°. Further, the Allahabad imager data show these waves to travel to the North-East direction. These observed wave parameters are summarized in Table 1.

3.2. 23–24 April 2009

Results of best-fit sinusoidal parametric estimation for the residual intensity data corresponding to 23–24 April 2009 are plotted in Fig. 5 for Gadanki O_2, OH and Allahabad OH data (top to bottom, respectively). Evident in the data are the short period wave features at both the locations. Over Gadanki, O_2 data exhibits ~2.8, 1.4 and 0.9 h waves to be the most dominant (top panel of Fig. 4) while

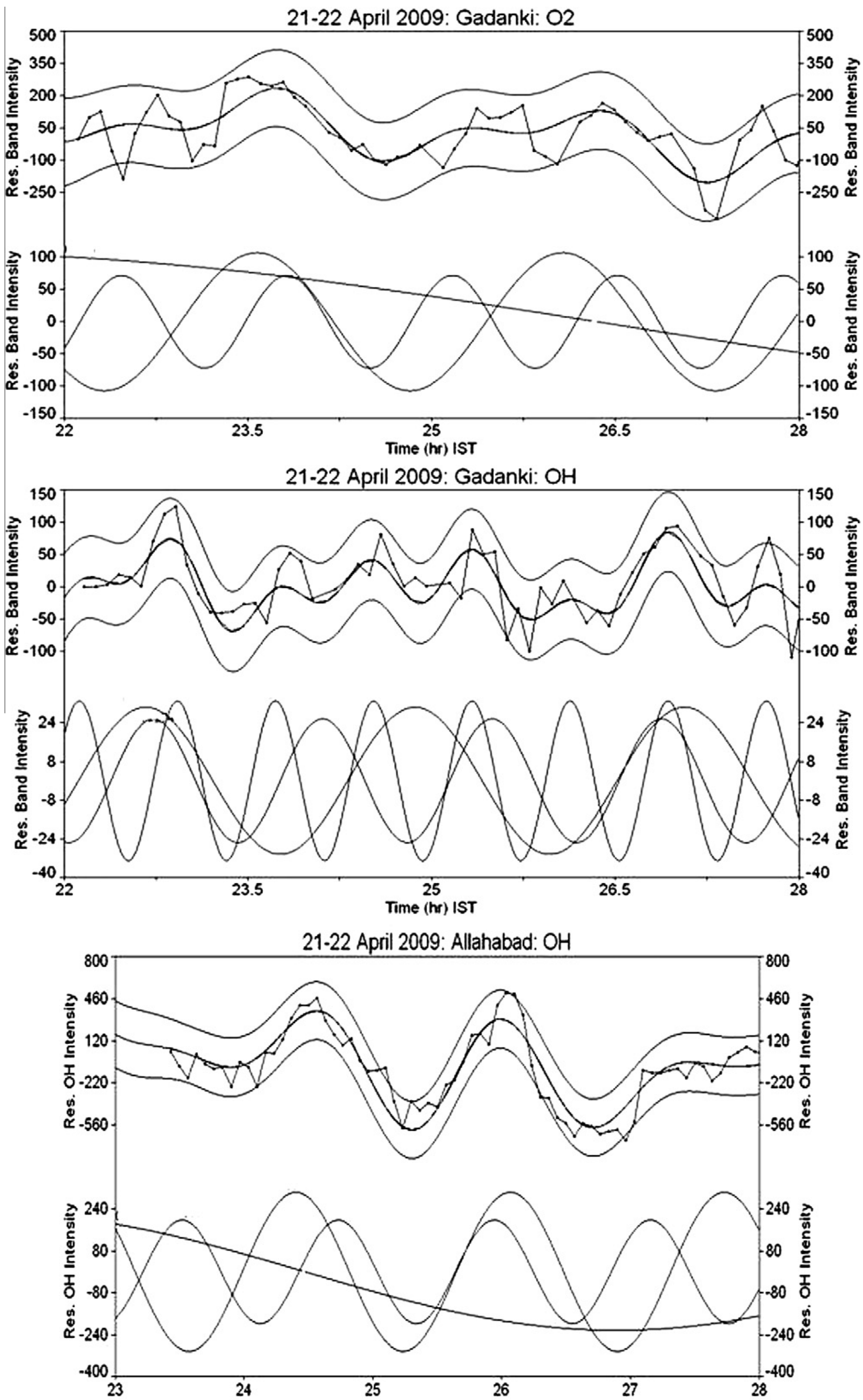

Fig. 4. Parametric best-fit model results for the mesospheric airglow observations of 21–22 April 2009. The top and middle panels show the results for O_2 and OH residuals of Gadanki observations, while bottom panel is shows the results for residuals of Allahabad OH data. In each panel plotted at the bottom is the variability of individual sinusoidal components while the resultants are plotted at the top with representative residual data.

the OH data show significant amplitudes for the ~3, 1.3 and 0.9 h waves. The upward propagation of waves is

c-
l-
e-
a-
r-
ly
n-
o-
t-
e-
d
in
d-
a-
ta

with a time delay of ~0.5 h (where cross correlation maxi-

Table 1
The estimated wave properties for Gadanki and Allahabad observations. Similar wave quantities are indicated by similar fonts.

Date	Gadanki			Allahabad	Wavelengths of common wave periods (km)	
	Wave periodicity (h)		Phase difference (h)	OH wave periodicity (h)	Vertical	Horizontal
	OH	O_2				
21–22 April 2009	~2, **1.3**, 0.8	~2, **1.2**	~0.6	~6.7, **1.4**, 0.8	~**12**	~**168**
23–24 April 2009	~3, **1.3**, *0.9*	~2.8, **1.4**, *0.9*	~0.5	~**1.5**, *0.8*, 0.6	~**12**, ~*22*	~**170**, ~*176*

mizes at ~0.91), which results in vertical group velocity ~18 km/h. The Allahabad data on the other hand exhibited dominant periodicity of ~1.5, 0.8 and 0.6 h. The commonality of two waves out of three dominant periodicities at both the places is an important aspect with regard to the spatial extent over which these short period gravity waves may propagate. As said earlier, assuming the vertical group velocity to represent the velocity of individual waves, the vertical wavelengths of ~1.4 and 0.9 h waves are estimated to be ~12 and 22 km, respectively. Therefore, the estimated horizontal wavelengths of these waves are ~170 and 176 km. This again shows the waves to propagate close to horizontal with angles of ~86° and 82° from their source regions. The Allahabad images show these waves to travel to the North-West.

4. Discussion

Our results clearly indicate the following characteristics in the mesospheric airglow emissions.

(a) On 21–22 April a wave with periodicity ~1.2 h was common to the Gadanki and Allahabad locations. The vertical and horizontal wavelengths of these waves were ~14 and 168 km, respectively. Also, the Gadanki data show that the 0.8 h wave was dissipated at ~94 km altitudes, but this wave was noted in the OH data at Allahabad.
(b) The 23–24 April data show 0.9 and 1.4 h waves to exist at both Gadanki and Allahabad locations with vertical wavelengths ~22 and 12 km and horizontal wavelengths of ~176 and 170 km, respectively.

To support the presence of above discussed wave signatures at both the locations; in Fig. 6, we plot version 1.07 temperature data averaged for the latitude and longitude range of 10–28° N and 75–85° E, obtained from the SABER instrument onboard the TIMED satellite (Remsberg et al., 2008). One may note the presence of a dominant wave with vertical wavelength of ~15 km on 21–22 April 2009 (Fig. 6a) while somewhat shorter vertical wavelengths (~12 km) were visible on 23–24 April 2009 (Fig. 6b), more-or-less similar to the observations made with the help of MLTP over Gadanki. Further, as noted in the ground based measurements and subsequent estimates, the apparent horizontal phase velocity of the waves on 21–22 April was ~40 m/s for ~1.2 h wave. Similarly the horizontal phase velocity of the 0.9 and 1.4 h waves is ~33 m/s and 54 m/s for 23–24 April 2009 data. These values are significantly higher than the typical background mesospheric wind amplitudes which vary from 10–30 m/s (as noticed in TIDI, onboard the TIMED satellite wind profiles for nearby nights, http://tidi.engin.umich.edu/) during April 2009. Therefore, it can be conjectured that these waves have overcome the mean wind filtering and reached long distances, noted as the common wave features at Gadanki and Allahabad. It is unfortunate that the TIDI winds were not available for the above mentioned nights to study the effects of winds on wave propagation. The dissipation of the 0.8 h wave at OH and O_2 altitudes is another interesting aspect. However, as this wave was observed in OH data from Allahabad, we feel that it may be ducted between OH and O_2 altitudes. To ascertain this, with horizontal wind model profiles and observed SABER temperature profiles over Gadanki we calculate the m^2 values (Fig. 7). Evident in the m^2 profile is a distinct region around 90–93 km altitudes where m^2 is negative. This region is defined as evanescent for the 0.8 h wave, i.e., the region where this wave can not propagate vertically (Chimonas and Hines, 1986). Surrounding this evanescent region there exist regions where m^2 is positive. The negative m^2 values may indicate a duct region where gravity waves can propagate to long distances at OH emission altitudes (~85–85 km) but were not observed at O_2 emission altitudes (~95 km). Though, we can not say whether it was Doppler duct or a thermal duct as the winds utilized are model only; a strong variation in the SABER temperature profile suggests a thermal duct.

Noteworthy is the presence of strong inversion layers in SABER temperature profiles on both the nights which again indicate the possibility of some of the waves getting trapped by a thermal duct, as suggested above. The unavailability of wind data limits our discussion of the dissipation of this wave within the 85–94 km altitude region and an estimate of mesospheric wind effects on the common waves observed at stations, horizontally separated by ~1200 km on both the nights of simultaneous observations. However, as noted in the OH and O_2 data of Gadanki, these waves were propagating upwards which shows them not to be ducted waves (except for the 0.8 h wave). It should be mentioned here that more statistics is required for a better understanding of the horizontal extent

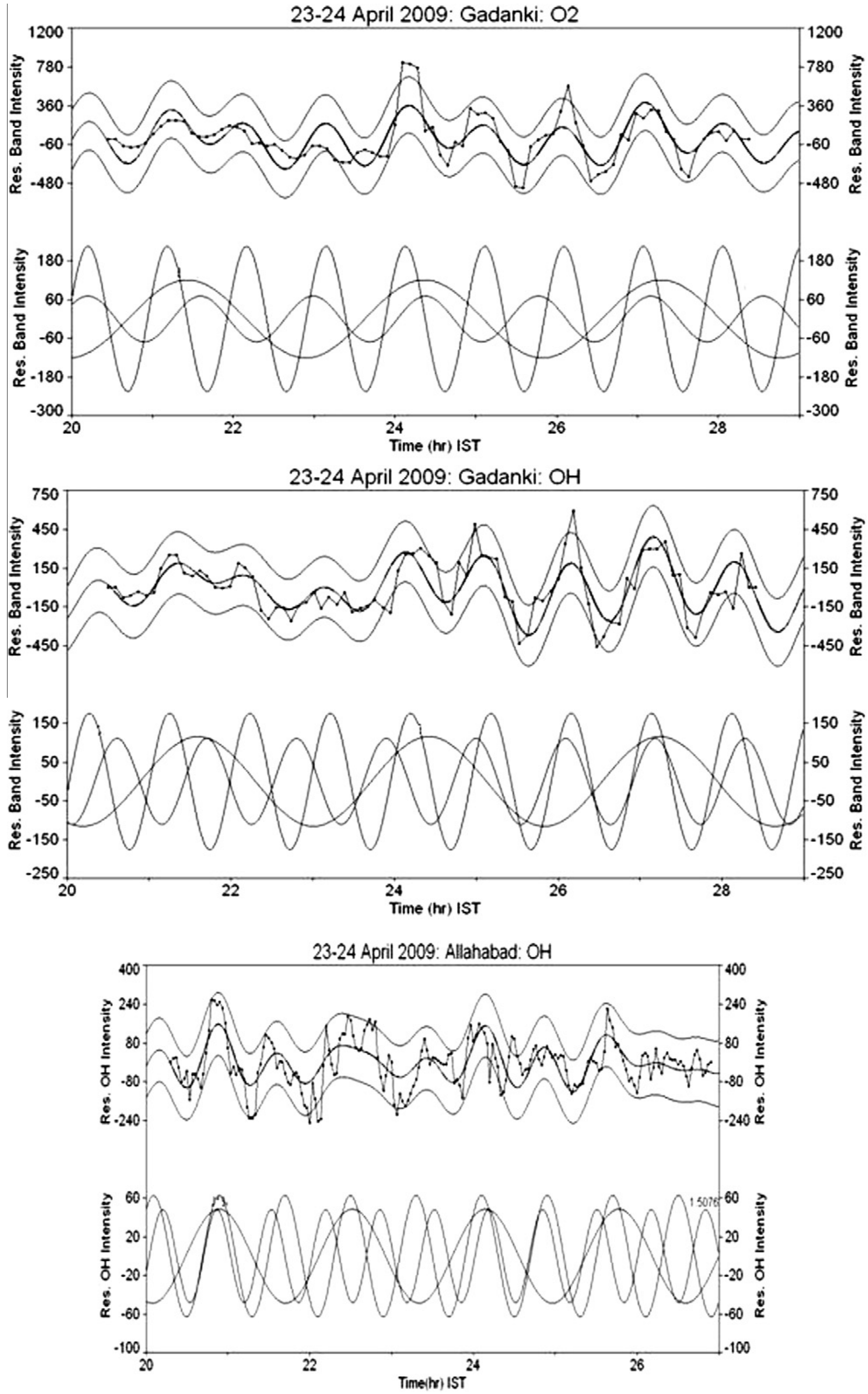

Fig. 5. Same as Fig. 4 but for the observations of 23–24 April 2009.

of waves and therefore the present case study is only indicative in nature.

There have been several reports suggesting that waves traveling to such large distances are signatures of ducted waves (e.g., Isler et al., 1997; Walterscheid et al., 2001; Snively and Pasko, 2008) while some reports also suggests that they may be upward propagating gravity waves and while propagating to greater heights, they may expand to larger spatial scales (Shiokawa et al., 2000). Our measurements show these waves to be upward propagating with a propagation angle very close to horizontal. Therefore,

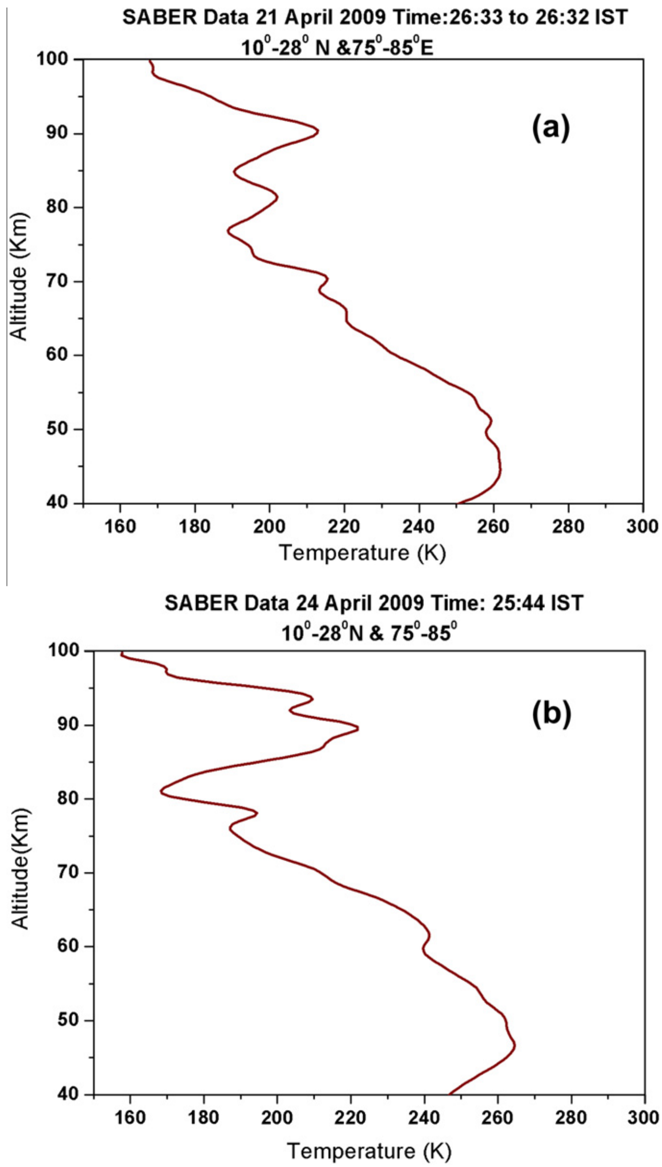

Fig. 6. Representative SABER temperature profiles over Gadanki for 21–22 and 23–24 April 2009. One may note wave signatures with vertical wavelengths from 10 to 25 km.

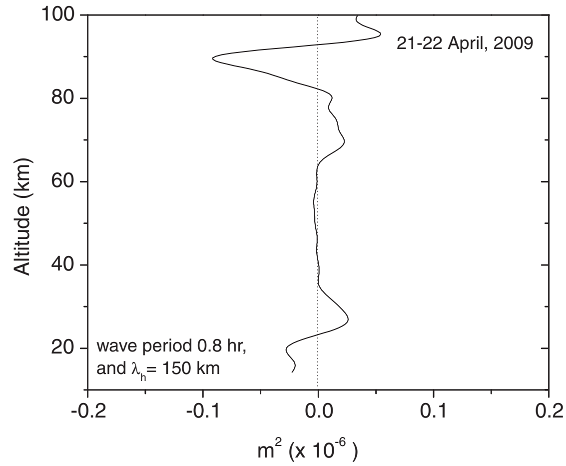

Fig. 7. The m^2 profiles calculated with the help of the horizontal wind model and SABER temperature and imager data. One may note a strong evanescent region for 0.8 h waves. The standing dotted lines show the zero values of m^2.

our results suggests that there exists a possibility for the observed plane wave fronts (as observed in some non-linear wave phenomena (Scheer and Reisin, 2010)) to be associated with upward propagating waves. However, these issues can not be resolved without multi-instrument, multi-station studies. To the best of our knowledge, there exist no reports from India with simultaneous bi-station mesospheric measurements. Therefore, our results are unique, nevertheless we report an interesting aspect of gravity wave propagation and effects, and multi-station studies, together with suitable wind information expected to become available via the upcoming NARL-SAFAR and NDMC programs, should shed more light on this subject.

Acknowledgments

A. Taori thanks the Director, NARL for his support of airglow research at NARL. The support of Mr. V. Kamalakar for airglow operation is duly acknowledged. This study is being carried out under the NARL – SAFAR and CAWSES India Phase II programs. The SABER data used in this study were obtained from http://saber.gats-inc.com. Authors thank Prof. B.R. Clemesha for his help in improving the manuscript content.

References

Chimonas, G., Hines, C.O. Doppler ducting of atmospheric gravity-waves. J. Geophys. Res. 91, 1219–1230, 1986.

Fritts, D.C. A numerical study of gravity wave saturation: nonlinear and multiple wave effects. J. Atmos. Sci. 42 (19), 2043–2058, 1985.

Fritts, D.C., Alexander, M.J. Gravity wave dynamics and effects in the middle atmosphere. Rev. Geophys. 41 (1), doi:10.1029/2001RG000106, 2003.

Fritts, D.C., Vadas, S.L., Riggin, D.M., Abdu, M.A., Batista, I.S., Takahashi, H., Medeiros, A., Kamalabadi, F., Liu, H.L., Fejer, B.G., Taylor, M.J. Gravity wave and tidal influences on equatorial spread F based on observations during the spread F Experiment (spreadFEx). Ann. Geophys. 26, 3235–3252, 2008.

Guharay, A., Taori, A., Bhattacharjee, S., Pant, P., Pandey, B., Pandey, K. First ground-based mesospheric measurements from central Himalayas. Current Sci. 9 (5), 664–669, 2009.

Hines, C.O. Internal gravity waves at ionospheric heights. Can. J. Phys. 38, 1441–1481, 1960.

Isler, J.R., Taylor, M.J., Fritts, D.C. Observational evidence of wave ducting and evanescence in the mesosphere. J. Geophys. Res. 102, 26301–26313, 1997.

Li, F., Liu, A.Z., Swenson, G.R. Characteristics of instabilities in the mesopause region over Maui, Hawaii. J. Geophys. Res. 110, doi:10.1029/2004JD005097, D09S12, 2005.

Lindzen, R.S. Turbulence and stress owing to gravity wave and tidal breakdown. J. Geophys. Res. 86, 9707–9714, 1981.

Mukherjee, G.K., Pragati Shikha, R., Parihar, N., Ghodpage, R., Patil, P.T. Studies of the wind filtering effect of gravity waves observed at Allahabad (25.45° N, 81.85° E). Earth Planets Space 62, 309–318, 2010.

Remsberg, E.E., Marshall, B.T., Garcia-Comas, M., et al. Assessment of the quality of the Version 1.07 temperature-versus-pressure profiles in the middle atmosphere from TIMED/SABER. J. Geophys. Res. 113, doi:10.1029/ 2008JD010013, D17101, 2008.

Scheer, J., Reisin, E.R. Statistical properties of nonlinear wave signatures in OH and O_2 airglow brightness data observed at lower midlatitudes. J. Atmos. Sol. Terr. Phys. 72, 588–594, 2010.

Shiokawa, K., Ejiri, M.K., Otsuka, Y., Ogawa, T., Kubota, M., Igarashi, K., Saito, A., Nakamura, T. Multi-point observation of short-period mesospheric gravity waves over Japan during the FRONT campaign. Geophys. Res. Lett. 27 (24), 4057–4060, 2000.

Smith, S.M., Scheer, J., Reisin, E.R., Baumgardner, J., Mendillo, M. Characterization of exceptionally strong mesospheric wave events using all-sky and zenith airglow observations. J. Geophys. Res. 111, doi:10.1029/2005JA011197. A09309, 2006.

Snively, J.B., Pasko, V.P. Excitation of ducted gravity waves in the lower thermosphere by tropospheric sources. J. Geophys. Res. 113, doi:10.1029/2007JA012693. A06303, 2008.

Taori, A., Dashora, N., Raghunath, K., Russell III, J.M., Mlynczak, Martin G. Simultaneous mesosphere, thermosphere–ionosphere parameter measurements over Gadanki (13.5° N, 79.2° E) – first results. J. Geophys. Res., under review

Taylor, M.J., Espy, P.J., Baker, D.J., Sica, R.J., Neal, P.C., Pendleton Jr, W.R. Simultaneous intensity, temperature, and imaging measurements of short period wave structure in the OH nightglow emission. Planet Space Sci. 39, 1171–1188, 1991.

Taylor, M.J., Turnbull, D.N., Lowe, R.P. Spectrometric and imaging measurements of a spectacular gravity wave event observed during the ALOHAH-93 campaign. Geophys. Res. Lett. 22, 2849–2852, 1995.

Tsunoda, R.T. On seeding equatorial spread F during solstices. Geophys. Res. Lett. 37, doi:10.1029/2010GL042576, L05102, 2010.

Walterscheid, R.L., Schubert, G., Brinkman, D.G. Small scale gravity waves in the upper mesosphere and lower thermosphere generated by deep tropical convection. J. Geophys. Res. 106 (D23), 31825–31832, 2001.

Yeh, K.C., Liu, C.H. The instability of atmospheric gravity waves through wave–wave interaction. J. Geophys. Res. 86, 9722–9728, 1981.